doi.org/10.36721/PJPS.2024.37.1.SP.235-243.1

Loading cinnamon oil into pH-sensitive chitosan grafted mesoporous silica nanoparticles via supercritical carbon dioxide

Huaping Lei[1,2], Yachao Jiang[1,2], Jinhua Liu[4], Youliang Guan[5], Songquan Song[3], Cuifang Tang[3], Sitian Fei[3] and Hui Zhang[1]*

[1]School of Pharmaceutical Sciences, Xiangnan University, Chenzhou, China
[2]Chenzhou Supercritical Carbon Dioxide Fluid Technology Research and Development Center, Xiangnan University, Chenzhou, China
[3]Nanling Research Institute for Modern Seed Industry, Xiangnan University, Chenzhou, China
[4]School of Chemistry and Environmental Sciences, Xiangnan University, Chenzhou, China
[5]The 705 Research Institute, China Shipbuilding Industry Corporation, Xi'an, China

Abstract: Stimulus-responsive mesoporous silica nanoparticles (MSNs) have displayed great potentiality for controlled-release and targeted drug delivery. In the current work, a supercritical fluid method was utilized to successfully prepare cinnamon oil loaded into chitosan grafted MSNs (CO@CS-MSNs). The influencing factors of drug loads, such as pressure, temperature, impregnation time and depressure time, were investigated. The structure of CO@CS-MSNs was demonstrated with Fourier-transform infrared (FT-IR) spectroscopy, transmission electron microscope (TEM), scanning electron microscopy (SEM), thermogravimetry (TG) as well as X-ray diffraction (XRD). The drug release assays *in vitro* at various pH conditions displayed that CO@CS-MSNs had an excellent pH-responsive release behavior, which confirmed that CO was loaded successfully into the CO@CS-MSNs. The findings indicated that the supercritical fluid approach is a non-destructive and efficient approach for stimulus-responsive MSNs, which is expected to further expand its application range.

Keywords: Supercritical carbon dioxide, mesoporous silica, nanoparticle, cinnamon oil.

INTRODUCTION

Its biodistribution ratio in pathogenic position directly influences the drug efficacy and its non-specific distribution in normal human organs and tissues may cause excessive toxicities or adverse reaction (Jia *et al*., 2019). As a result, controlled-release and targeted nano drug delivery systems have been recognized as an excellent medical strategy, particularly in the research of cancer treatment research (Srinivasarao and Low, 2017; Bahrami *et al*., 2017; Küçüktürkmen and Rosenholm, 2021). Stimulus-responsive mesoporous silica nanoparticles (MSNs) have aroused much attention in controlled and targeted nano drug-delivery systems on account of their narrow distribution of particle size, large specific surface area, excellent biocompatibility together with stable structure (Wen *et al*., 2017; Song *et al*., 2017; Li *et al*., 2021).

Different kinds of stimulation-responsive MSNs have been widespread investigated and may reveal significant 'switch on/off' function in response to certain endogenous stimuli, for instance reduced pH (Jia *et al*., 2019; Feng *et al*., 2018), certain enzymes (Tukappa *et al*., 2016), excess glutathione (redox-sensitive) (Wang *et al*., 2015), or overexpression of adenosine triphosphate (ATP) (Lai *et al*., 2015). Nevertheless, it remains a huge challenge to encapsulate the drugs into the pores of functional MSNs containing good safety, efficacy and stability.

**Corresponding author:* e-mail: audenlei@163.com

In general, drugs were loaded prior to surface stimulus-responsive modifications (namely, the process of 'gate install') since the great majority of 'gate-open' actions are irreversible (for instance, disulfide bond breakage in the redox-sensitive systems) (Chen *et al*., 2017; Cheng *et al*., 2017). As a result, in the grafting process of covalent polymer, the drugs may be contaminated by the reactants, leak, and even undergo chemical reactions. After polymer-grafting, the drug loading can avoid these shortcomings, but only if the 'gate-open' action was reversible. These approaches are mainly seen in some researches of pH-sensitive MSNs, whose 'gate' can be repeatedly switched on and off in accordance with various pH values (Abbaszad *et al*., 2016; Guo *et al*., 2017; Esmaeili *et al*., 2022; Ghahfarokhi *et al*., 2022). Nonetheless, the model drugs utilized in these researches must be hydrophilic, owing to the free diffusion of drugs into particles at low pH requires an aqueous environment. The defects of the existing drug delivery pathways have caused great restrictions on the progress of stimulus-responsive mesoporous silica nanoparticles. A safer, more efficient and more widely applied drug delivery strategy is expected.

Carbon dioxide supercritical fluid technique may be an alternative to stimulus-responsive MSNs for the drug delivery for the subsequent reasons. Numerous natural active ingredients possess considerable solubility in the supercritical CO_2. Thus, supercritical CO_2 can be applied as a convenient carrier to transport drugs into nanocarriers

and there is no residual solvent in the ultimate product. Second, supercritical CO_2 has almost no interfacial tension, is extremely permeable and easily passes through polymer network architectures (Jia *et al*., 2019). Additionally, it could be observed that the supercritical CO_2 can decrease the forces in the molecule between macromolecules when the molecules of CO_2 are inserted into nanoscale gaps (Padmajan *et al*., 2016; Jia *et al*., 2016). These special performances of supercritical CO_2 allow the drug to be transported directly into the polymer-grafted MSNs via a closed 'gates' in the absence of any impurity introduction and structural injury (Ajiboye *et al*., 2022).

Hence, we attempted to load the pharmaceutical components into chitosan grafted MSNs (CS-MSNs) in a direct gate-permeable manner with the assistance of carbon dioxide. As described earlier, it is difficult for hydrophobic components to enter the gated architecture by conventional routes, thus cinnamon oil (CO), a multicomponent essential oil, was chosen as template drug.

CO possesses a wide range of pharmacological activities, for instance anti-bacterial, anti-ulcer and anti-tumor effects (Ka *et al*., 2003) and has been generally applied in the area of traditional Chinese medicine. CO inhibited tumor growth by reducing tumor cell count, viability and proliferation accompanied by the inhibition of tumor growth rate (Morsi *et al*., 2022). Cinnamaldehyde, the main component of cinnamon oil, can inhibit the proliferation of tumor cells by inducing reactive oxygen species to mediate mitochondrial membrane osmotic transformation and promoting the release of cytochrome C (Ka *et al*., 2003).

There are no reports of CO loading into CS-MSNs. The selection of multi-component CO can examine the applicability of our approach as much as possible. This research was conducted to develop a gate-penetration method for directly loading drugs into stimulus-responsive CS-MSNs and to assess the non-destructivity and feasibility of the approach by studying drug release behavior, morphological structure characterization and drug loading.

MATERIALS AND METHODS

Materials

Cinnamon oil produced by steam distillation was supplied by the Jiangxi Hairui Natural Plant Limited Company (Jiangxi Province, China) and cinnamaldehyde was provided by Hubei Province Kangchun Perfume Co., Ltd. (Hubei Province, China). MCM-41 mesoporous silica was purchased from Beijing Beike 2D materials Co., Ltd. Chenzhou Guoneng Gas Co., Ltd (Hunan Province, China) provided the high-purity CO_2 (99.99%). All of the other chemicals were of analytical grade.

Preparation of chitosan grafted MCM-41 mesoporous silica nanoparticles (CS-MSNs)

The synthesis method of CS-MSNs was as reported via Xiaoxi Hu, etc (Hu *et al*., 2014). Commonly, at first, 10.0 g chitosan was added into an aqueous solution of 1000 mL acetic acid (5 wt%). After one day of magnetic stirring (1300rpm) under ambient temperature, a transparent chitosan solution (1% w/v) was produced, which could be applied for the following coating step. Simultaneously, 5.0g powdered MSNs were dispersed in 500mL ethanol through ultrasonic for 15mins and acetic acid was added for adjusting the pH to approximately 4.0. At ambient temperature, 5.0g GPTMS was rapidly added into MSNs-in-EtOH solvent through magnetic stirring (500 rpm) for 3h. 1000mL produced chitosan solution was added into the mixture and subsequently stirred for one day at ambient temperature to obtain CS-MSNs. Such CS-MSNs were gathered through centrifugation (7000 rpm), washed 3 times utilizing ethanol and deionized water, and allowed to dry overnight at 50℃ in vacuum drying oven.

Generation of CO@CS-MSNs

The instruments utilized in this work were the same as those mentioned in the literature (Jia *et al*., 2019). Commonly, CS-MSNs (1.0g) are placed in a stainless steel basket with a dense stainless steel mesh at the bottom. The basket was next suspended and sealed in a 70.7mL volume (with the inner diameter and height of 3cm and 10cm) loading chamber. The loading chamber was injected with CO (5mL) through the inner wall of the coaxial nozzle (i.d.120μm) with a high-pressure constant-current pump and CS-MSNs were immersed in CO for a period of time. The carbon dioxide was simultaneously transported with a high-pressure pump, heated through an electric preheater, and sent to the charging chamber via an external nozzle. CO_2 was transported continuously prior to the pressure increased to a preset value and the high pressure was maintained for a given time to load CO into CS-MSNs. In the end, a depressurization operation for a certain time was carried out and the CO_2 was slowly discharged. Eventually, the finished product CO@CS-MSNs were removed and blown dry with micro nitrogen for 5 mins with an aim of removing external CO.

Characterization

A transmission electron microscope (TEM) (JEM-2010 (HR) 200kv, JEOL, Japan) and scanning electron microscope (SEM) (Sus5000, Hitachi Company, Japan) were applied for observing the morphologies of CO@CS-MSNs, CS-MSNs together with MSNs. The internal pore architectures of MSNs were implemented with the measurements of BET and a surface area and pore analyzer (TriStar α, Micromeritics Co., Ltd., USA) was exploited for drawing the nitrogen-adsorption-desorption isotherms. The particle size and Zeta potential of MSNs, CS-MSNs and CO@CS-MSNs were measured by Nano particle size and Zeta potential analyzer (Nano-ZS90, Malvern, UK). The samples were dispersed with ultra-

pure water, ultrasonic for 5mins and then determined. The pH value for Zeta potential measurement was 7.0.

Utilizing the X-ray diffractometer (UItimaχ, Rigaku Company, Japan), PXRD patterns were acquired. Such patterns were commonly collected over 2θ at 3-10°. FT-IR spectrophotometer (Cary 630 FTIR, Agilent Corporation, USA) was utilized for acquiring FT-IR transmission spectra with KBr discs in 4000 to 400 cm^{-1} region. TGA was implemented with thermogravimetry (DSC-TGA SDT 650, TA Corporation, USA) from 40□ to 800□ under N_2 atmosphere.

Determination of drug loads (DLs)

The CO composition was explored utilizing a GC-2010 pro gas chromatograph with FID detector and a Wonda Cap 5 chromatographic column (30m×0.25 mm×0.25μm) (Shimadzu Company, Japan). The temperature of detector and injector were 220 and 200°C, respectively. N_2 was applied as the carrier gas at a flow rate of 2.0mL min^{-1}. Under a splitting condition, the sample (2.0μL) was injected at 20:1 splitting ratio. The temperature of oven was set to 100°C and subsequently programmed at 5□ min^{-1} to 150□ for five mins, then at 5□ min^{-1} to 200□ and held for 5mins. Vanilline was selected as internal standard to quantify cinnamaldehyde.

DLs of cinnamaldehyde of CO in CO@CS-MSNs were detected as below. In short, CO@CS-MSNs (20mg) was ultrasonically treated in 2mL of acidic EtOH (pH adjusted with acetic acid to approximately 4.0) for 120mins to completely release the trapped CO. Subsequently, the analysis of samples was performed with GC after filtration and the DLs of CO could be calculated as below:

$$DL = \frac{m}{m_{CO@CS-MSNs}} \times 100\%$$

m represented the entrapped mass of CO in solution CO@CS-MSNs. $m_{CO@CS-MSNs}$ represented the CO@CS-MSNs mass.

In vitro release of CO

The solution of phosphate buffered saline (PBS, 250mL) was added with CO@CS-MSNs (500mg), where the pH of 1% Tween 80 was 7.0 and 5.8, respectively and stirred (50 rpm) in a 37.5°C water bath slowly. The aqueous samples (1.0mL) were extracted from the same water level at various time intervals and PBS (1.0mL) was immediately added after each extraction. The acquired samples were filtered and the filtrate was extracted with 4 mL of ethyl acetate and 1mL of internal standard (Vanilline), shaken well, stood and the supernatant was taken for GC analysis. The GC conditions were the same as the part of determination of drug loads.

Thermal stability evaluation

The thermal stability of CO@CS-MSNs was evaluated with reference to the method reported by Guo Tao *et al.* (Guo *et al.*, 2000). CO@CS-MSNs and the physical mixture of CO and CS-MSNs of 2.0 g each were weighed, and placed in an environment of 50% relative humidity at constant temperature conditions of 60°C and 80°C for 24 h, respectively. The sample (20mg) was extracted at 1, 2, 4, 8, 12 and 24h, immediately dissolved in 25mL acidic EtOH with pH 4.0 (plus 1mL vanillin internal standard solution) for ultrasound for 2h and filtered with 0.45μm microporous filter membrane. The sample was used as the test solution for GC analysis. The GC conditions were the same as the part of determination of drug loads.

STATISTICAL ANALYSIS

The software for statistical analysis of standard deviation is Microsoft Excel 2007.

RESULTS

Preparation of CO@CS-MSNs

AS shown in table 1, samples Nos.1-3 was prepared with different pressures. The drug loads increased obviously along with pressures. As shown in samples Nos.4-5 and No.2, the drug loads decreased along with temperature from 35° to 45° but increased at 55 °. From samples Nos.6-7 and sample No.2, the drug loads increased gradually along with impregnation time from 15 mins to 45 mins. The drug loads decreased with depressure time increasing from samples no.8-9 and sample No.2.

Characterization of MSNs, CS-MSNs and CO@CS-MSNs

Particle morphology

CO@CS-MSNs, CS-MSNs as well as MSNs morphology could be observed with TEM and SEM, the images are displayed in fig. 1. In fig. 1A and 1B, the SEM outcomes revealed that the inordinance adhesive particles with rough surface were acquired and TEM view displayed the mesoporous structure. In comparison with the MSNs relative sparsity, the SEM image of CS-MSNs in fig. 1C revealed that CS-MSNs particles were closer, which was created with grafted chitosan branches. The TEM image of CS-MSNs in fig. 1D reveals that the internal mesoporous architecture of MSNs was still intact. SEM together with TEM images for the CO@CS-MSNs were shown in fig. 1E and 1F. There existed no difference between the CS-MSNs and CO@CS-MSNs in terms of internal structure and surface morphology

The BET structure parameters of CO@CS-MSNs, CS-MSNs together with MSNs were showed in table 2. CS-MSNs revealed a lager BET surface area in comparison with that of CO@CS-MSNs and MSNs, attributing to grafted chitosan branches. After loading CO, the pore volume decreased markedly. The pore sizes became a little larger after grafting chitosan branches and loading drug. fig. 2 displayed the N_2-adsorption-desorption isotherms, indicating CO@CS-MSNs and CS-MSNs had much more quantity absorbed of nitrogen than that of MSNs.

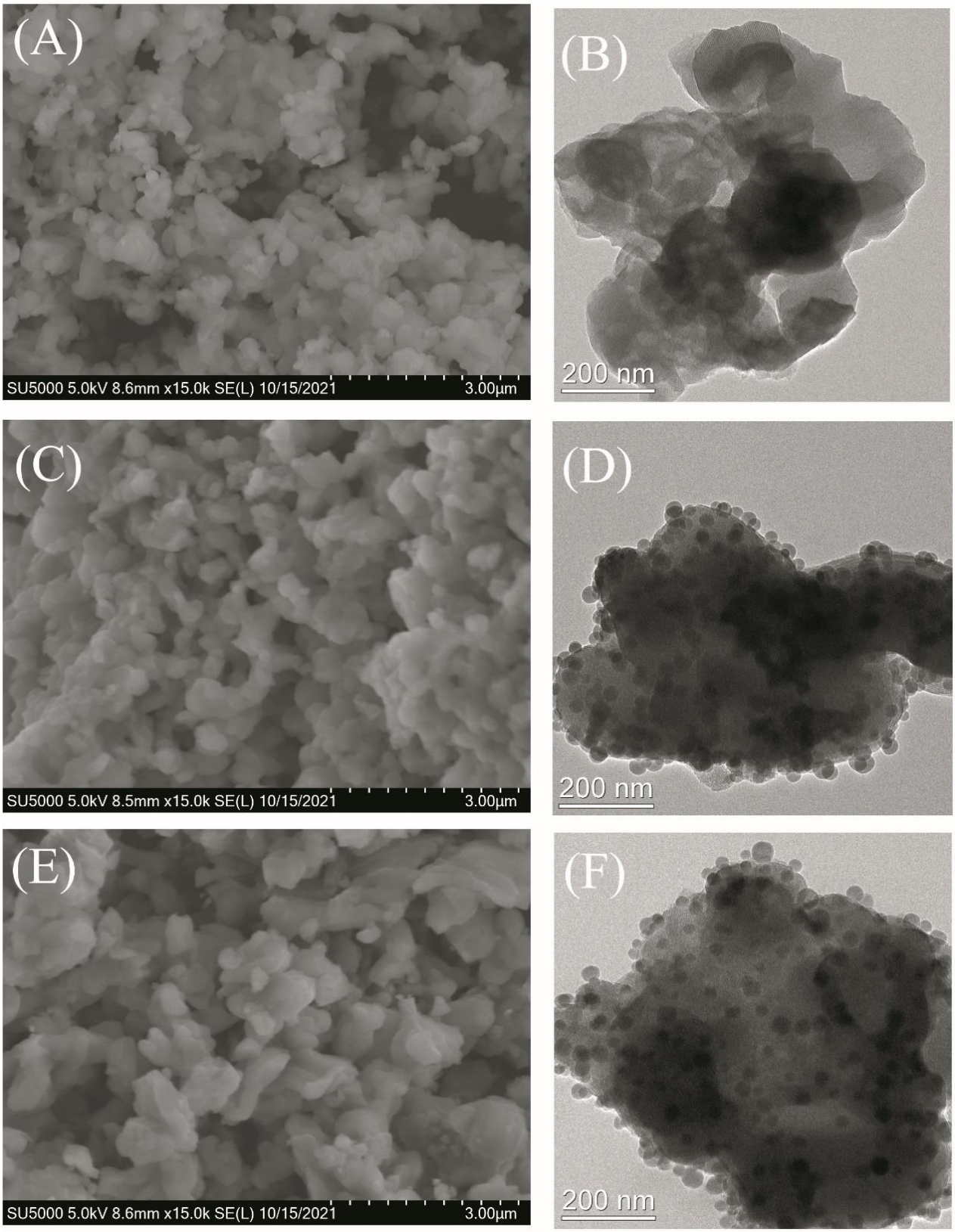

Fig. 1: Morphology of mesoporous silica nanoparticles (MSNs) observed by (A) scanning electron microscope (SEM) and (B) transmission electron microscope (TEM), chitosan grafted MSNs (CS-MSNs) by (C) SEM and (D) TEM, and that of cinnamon oil loaded CS-MSNs (CO@CS-MSNs) by (E) SEM and (F) TEM.

Table 1: Drug load for cinnamon oil loaded chitosan grafted mesoporous silica nanoparticles (CO@CS-MSNs) under different operation conditions (n=3)

Sample no.	P(MPa)	T(ºC)	Impregnation time (min)	Depressure time (min)	Drug load (%)
1	10	45	30	10	7.9±1.1%
2	15	45	30	10	31.3±1.4%
3	20	45	30	10	37.5±1.3%
4	15	35	30	10	33.6±0.9%
5	15	55	30	10	35.4±1.5%
6	15	45	15	10	21.9±1.2%
7	15	45	45	10	34.7±2.1%
8	15	45	30	5	33.2±1.7%
9	15	45	30	15	28.7±1.6%

Table 2: The Brunauer-Emmett-Teller (BET) structure parameters of mesoporous silica nanoparticles (MSNs), chitosan grafted mesoporous silica nanoparticles (CS-MSNs) and cinnamon oil loaded CS-MSNs (CO@CS-MSNs)

Iterms	MSNs	CS-MSNs	CO@CS-MSNs
BET surface area (m^2/g)	37.1524	1,086.7165	5.8987
Pore volume (cm^3/g)	0.3534	0.5916	0.03159
Average pore size (nm)	3.0649	3.2237	5.0329

Table 3: Average particle size and zeta potential of mesoporous silica nanoparticles (MSNs), chitosan grafted mesoporous silica nanoparticles (CS-MSNs) and cinnamon oil loaded CS-MSNs (CO@CS-MSNs) (n=3)

Samples	Average particle size (nm)	Zeta potential (mV)
MSNs	212.23±4.00	-21.77±0.74
CS-MSNs	314.33±14.53	-5.64±1.15
CO@CS-MSNs	516.13±7.83	-4.89±0.57

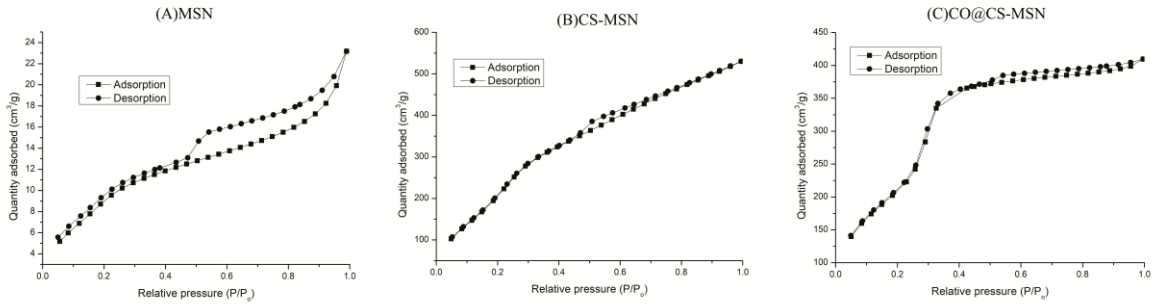

Fig. 2: Nitrogen-adsorption–desorption isotherms of (A) mesoporous silica nanoparticles (MSNs), (B) chitosan grafted MSNs (CS-MSNs) and (C) cinnamon oil loaded CS-MSNs (CO@CS-MSNs).

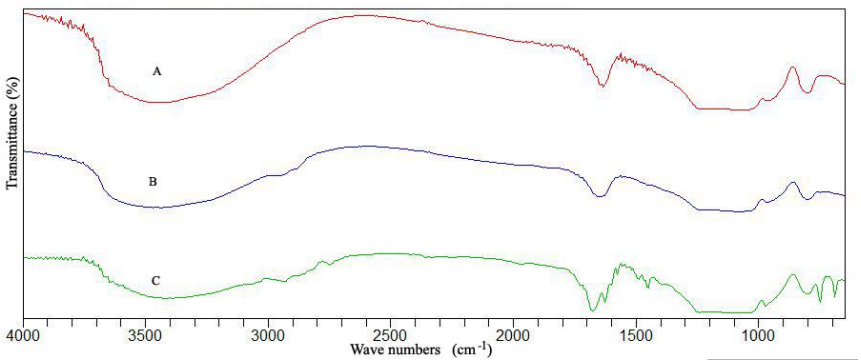

Fig. 3: Fourier transformed infrared (FT-IR) spectroscopy of (A) mesoporous silica nanoparticles (MSNs), (B) chitosan grafted MSNs (CS-MSNs) and (C) cinnamon oil loaded CS-MSNs (CO@CS-MSNs).

Particle size and zeta potential analysis

As shown in table 3, after chitosan modification, the particle size of mesoporous silica changed from 212.23±4.00 nm to 314.33±14.53 nm. This proved that chitosan successfully modified mesoporous silicon and increased the particle size of mesoporous silica. After loading CO, the particle size further increased to 516.13± 7.83 nm, indicating that the CO was successfully loaded.

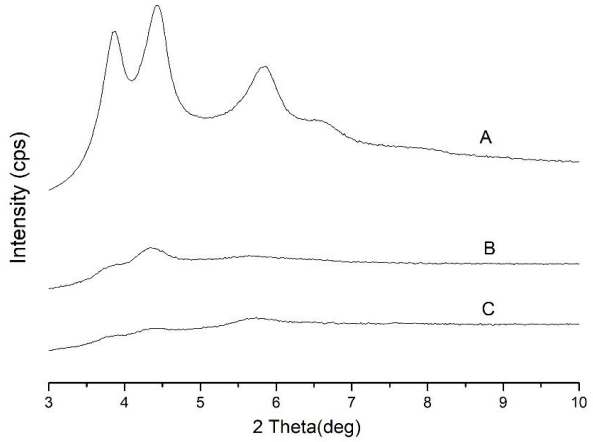

Fig. 4: XRD patterns of (A) mesoporous silica nanoparticles (MSNs), (B) chitosan grafted MSNs (CS-MSNs) and (C) cinnamon oil loaded CS-MSNs (CO@CS-MSNs).

Due to the large amount of Si-OH on the surface, MSNs presented a negative potential (-21.77± 0.74 mV), and after chitosan modification, the potential became -5.64± 1.15 mV. This is because chitosan contains a positively charged amino group, which neutralizes part of the negative charge of MSNs, resulting in an increase in potential. These results indicate that MSNs is successfully modified by chitosan. There was little change in potential after loading CO.

FT-IR characterization

FT-IR spectroscopy of CO@CS-MSNs, CS-MSNs together with MSNs were determined, as exhibited in fig. 3. The peaks present at 2925 and 2981cm^{-1} represented the characteristic absorption of C-H stretching in the curve of CS-MSNs (fig. 3B) in contrast to MSNs (fig. 3A) (Dimzon and Knepper, 2015). In the spectrum of CO@CS-MSNs, the major CO components created a large amount of the characteristic peaks. For instance, in fig. 3C the peak at 1643cm^{-1} revealed the signal of unsaturated aldehyde. And many characteristic peaks appeared near 1500 and 800cm^{-1}, which were obviously different from fig. 3A and fig. 3B.

Powder XRD patterns

Based on fig. 4A, the MSNs XRD pattern shows a series of peaks, which means that it has crystal characteristics. By comparison, the patterns generated by CS-MSNs and CO@CS-MSNs can be found that chitosan grafting and CO loading to the mesoporous silica nanoparticles, significantly lowered the height of the diffraction peaks.

TG characterization

In fig. 5, TG analysis was performed under an atmosphere of N_2 to explore the samples' composition ratio. The weight loss rates of CO@CS-MSNs, CS-MSNs together with MSNs were 36.0%, 18.7% and 13.2%, respectively.

In vitro drug release of CO@CS-MSNs and its stimulus-response to pH

The cumulative release curves of CO in fig. 6 clearly displayed the release behavior of CO in stimulus-response to pH in CS-MSNs. As the pH decreased from 7.0 to 5.8, the cumulative release rate of CO increased obviously.

Thermal stability evaluation of CO@CS-MSNs and its physical mixture

It can be clearly seen from fig. 7 that the release rate of CO@CS-MSNs was lower than that of the physical mixture at various times at 60□ and 80□ and the stability of CO loaded into CS-MSNs was significantly improved.

DISCUSSION

Loading cinnamon oil into chitosan grafted mesoporous silica nanoparticles via supercritical carbon dioxide, on one hand, compared with the gas phase, the interfacial tension of supercritical CO_2 is very small, which makes supercritical CO_2 have powerful permeability and can

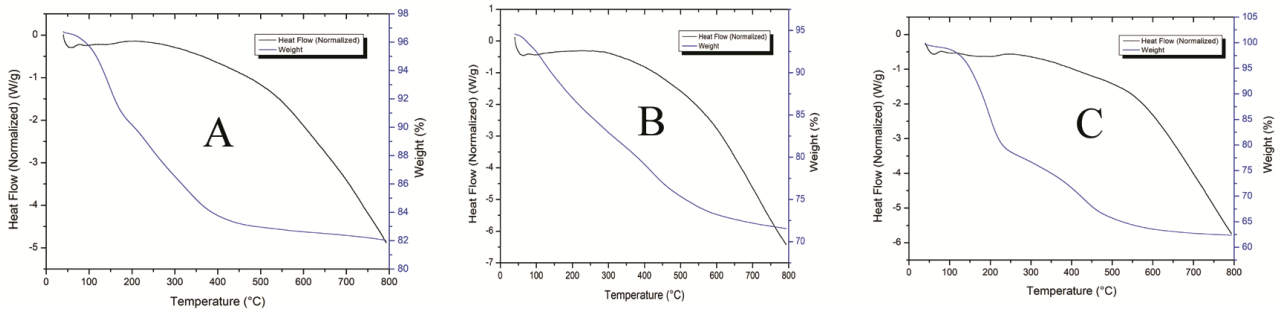

Fig. 5: Thermogravimetric (TG) analysis of (A) mesoporous silica nanoparticles (MSNs), (B) chitosan grafted MSNs (CS-MSNs) and (C) cinnamon oil loaded CS-MSNs (CO@CS-MSNs).

penetrate with chitosan branches. On the other hand, when supercritical CO_2 is inserted into gaps between the branches of chitosan, the intermolecular forces will be weakened, so that the 'gate' of CO entry is relatively loose (Jia *et al.*, 2019).

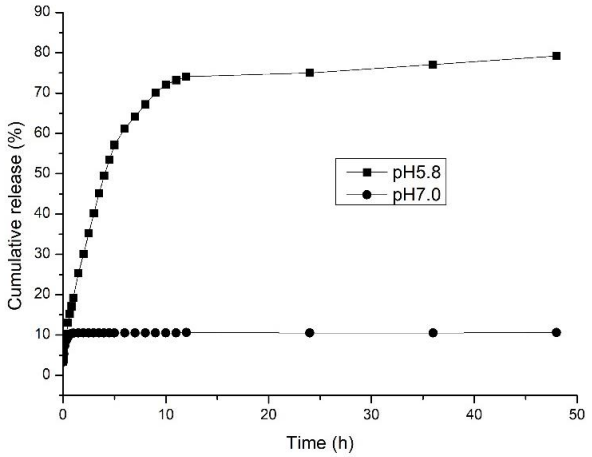

Fig. 6: *In vitro* release from of cinnamon oil loaded chitosan grafted mesoporous silica nanoparticles (CO@CS-MSNs) in phosphate buffered saline (PBS) of pH 7.0 and pH 5.8.

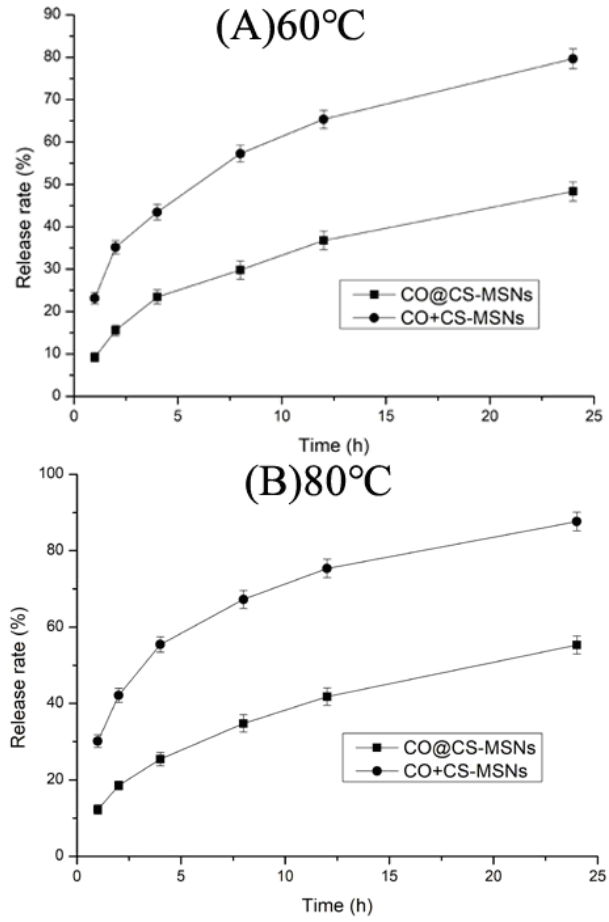

Fig. 7: Thermal stability evaluation of cinnamon oil loaded chitosan grafted mesoporous silica nanoparticles (CO@CS-MSNs) and its physical mixture (CO+CS-MSNs) at (A) 60º and (B) 80 º (n=3).

The density of CO_2 increased when pressure increased, which may help dissolve CO in supercritical CO_2, followed by permeation of the supercritical solution into CS-MSNs and precipitated CO inside CS-MSNs. As temperature rising, the density of CO_2 decreased, which may be against dissolving CO in supercritical CO_2 and precipitating CO inside CS-MSNs. On the other hand, temperature increased from 35º to 55º may result in intensifying thermal motion of the molecules which help to improve loading CO into CS-MSNs. It is obvious that the drug loading by supercritical CO_2 method required a certain period of time, because the diffusion of CO/CO_2 loading phases in polymer chitosan and mesoporous silica nanopore channels took a certain time. The drug loads decreased with depressure time increasing. It may be due to CO freeing from CS-MSNs in depressure process.

SEM together with TEM images showed there existed no difference between the CS-MSNs and CO@CS-MSNs in terms of internal structure and surface morphology, suggesting that the drug loading approach is non-destructive. In FT-IR spectroscopy, the peaks present at 2925 and 2981 cm^{-1} represented the characteristic absorption of C-H stretching in the curve of CS-MSNs in contrast to MSNs (Dimzonn and Knepper, 2015). The results suggested that chitosan branches were grafted successfully on the MSNs surface. And many characteristic peaks appeared near 1500 and 800cm^{-1} in the curve of CO@CS-MSNs, indicating that CO has been incorporated into chitosan grafted mesoporous silicon materials to form new chemical bonds. These results prove that CO has been successfully loaded into the CS-MSNs particles. By comparison, the XRD patterns generated by MSNs, CS-MSNs and CO@CS-MSNs can be found that chitosan grafting and CO significantly lowered the height of the diffraction peaks, this is due to that the introduction of the organic functional groups decreased the crystallinity of the sample and after organic groups loading the crystal lattice structure and arrangement of the sample has changed. In TG analysis, the weight loss rates of CO@CS-MSNs, CS-MSNs together with MSNs were 36.0%, 18.7% and 13.2%, respectively. The results showed that CO could be effectively loaded into chitosan grafted mesoporous silicon materials.

The cumulative release curves of CO showed as the pH decreased from 7.0 to 5.8 the cumulative release rate of CO increased obviously. These results indicated that CO@CS-MSNs have the performance of pH controlled release.

As-formed CO@CS-MSNs may be a new drug delivery system for underlying pH-sensitive release control and targeting for CO clinical uses. The developed CO@CS-

MSNs may be therapeutic applied in leukemia, lung cancer and prostate cancer (Morsi *et al*., 2022; Ka *et al*., 2003).

CONCLUSION

In this work, CO was loaded into CS-MSNs directly through chitosan branching by supercritical CO_2 approach, with high efficiency and no structural damage. The structure characterization and morphology of FT-IR, TEM, SEM, TG and XRD, together with particle size and Zeta potential analysis proved that CO permeated the 'gate' and loaded into internal channel of CS-MSNs. The temperature, pressure, depressure and impregnation time, as well as other procedure parameters were explored. The best process conditions are impregnation pressure 20 MPa, impregnation temperature 45ºC, impregnation time 30mins and depressure time 10 mins. In the best process conditions CO@CS-MSNs of DL more than 35% was obtained. The in vitro drug release assay shown that CO@CS-MSNs achieves pH-sensitive controlled release. Thermal stability evaluation proves that the stability of CO loaded into CS-MSNs was significantly improved. This work evidently displays that the supercritical CO_2 approach is a promising drug loading strategy for the preparation of controlled-release and targeted novel drug delivery systems, which could be applied for more hydrophobic drugs or other gated mesoporous nanocarriers.

ACKNOWLEDGEMENTS

The authors extend their appreciation to The Natural Science Foundation of Hunan Province China (Grant No. 2021JJ30639 and 2021JJ80074), Ministry of Education of Hunan Province China (Grant No. 19B524) and Provincial Special Project of Chenzhou National Sustainable Development Agenda Innovation Demonstration Zone Construction (Grant No. 2022sfq06).

REFERENCES

Abbaszad Rafi A, Mahkam M, Davaran S and Hamishehkar H (2016). A Smart pH-responsive Nano-Carrier as a Drug Delivery System: A hybrid system comprised of mesoporous nanosilica MCM-41 (as a nano-container) & a pH-sensitive polymer (as smart reversible gatekeepers): Preparation, characterization and in vitro release studies of an anti-cancer drug. *Eur. J. Pharm. Sci.*, **93**: 64-73.

Ajiboye AL, Jacopin A, Mattern C, Nandi U, Hurt A and Trivedi V (2022). Dissolution improvement of progesterone and testosterone via impregnation on mesoporous silica using supercritical carbon dioxide. *AAPS Pharm. Sci. Tech.*, **23**(8): 302.

Bahrami B, Hojjat-Farsangi M, Mohammadi H, Anvri A, Ghalamfarsa G, Yousefi M and Jadidi-Niaragh F (2017). Nanoparticles and targeted drug delivery in cancer therapy. *Immunol. Lett.*, **190**: 64-83.

Chen XL, Sun H, Hu J, Han X, Liu HL and Hu Y (2017). Transferrin gated mesoporous silica nanoparticles for redox-responsive and targeted drug delivery. *Colloids Surf B Biointerfaces.*, **152**: 77-84.

Cheng W, Liang CY, Wang XS, Tsai J, Liu G, Peng YM and Nie JP (2017). A drug-self-gated and tumor microenvironment-responsive mesoporous silica vehicle: "four-in-one" versatile nanomedicine for targeted multidrug-resistant cancer therapy. *Nanoscale*, **9**(43): 17063-17073.

Dimzon IK and Knepper TP (2015). Degree of deacetylation of chitosan by infrared spectroscopy and partial least squares. *Int. J. Bio. Macromol.*, **72**: 939-945.

Esmaeili Y, Khavani M, Bigham A, Sanati A, Bidram E, Shariati L, Zarrabi A, Jolfaie NA and Rafienia M (2022). Mesoporous silica@chitosan@gold nanoparticles as "on/off" optical biosensor and pH-sensitive theranostic platform against cancer. *Int. J Biol. Macromol.*, **202**: 241-255.

Feng LZ, Dong ZL, Tao DL, Zhang YC and Liu Z (2018). The acidic tumor microenvironment: A target for smart cancer nano-theranostics. *Natl. Sci. Rev.*, **5**(2): 269-286.

Ghahfarokhi MR, Dini G and Movahedi B (2022). Fabrication of chitosan-coated mesoporous silica nanoparticles bearing rosuvastatin as a drug delivery system. *Curr. Drug Deliv.*, **19**(1): 64-73.

Guo T, Song HT, Yang XT, Yu KJ and Zhang RH (2000). Study on the stability of β-cyclodextrin inclusion complexes of cinnamon oil. *Chin. J. Chin. Mater. Med.*, **25**(7): 27-29.

Guo YM, Li H, Shi WK, Zhang J and Feng J (2017). Targeted delivery and pH-responsive release of doxorubicin to cancer cells using calcium carbonate/hyaluronate/glutamate mesoporous hollow spheres. *J. Colloid Interface Sci.*, **502**: 59-66.

Hu XX, Wang Y and Peng B (2014). Chitosan-capped mesoporous silica nanoparticles as pH responsive nanocarriers for controlled drug release. *Chem. Asian J.*, **9**(1): 319-327.

Jia JF, Gai YZ, Wang WC and Zhao YP (2016). Green synthesis of biocompatiable chitosan-graphene oxide hybrid nanosheet by ultrasonication method. *Ultrason. Sonochem.*, **32**: 300-306.

Jia JF, Liu XJ, Wu KY, Zhou X and Ge FH (2019). Loading zedoary oil into pH-sensitive chitosan grafted mesoporous silica nanoparticles via gate-penetration by supercritical CO_2 (GPS). *J. CO_2 Util.*, **33**: 12-20.

Ka H, Park HJ, Jung HJ, Choi JW, Cho KS, Ha J and Lee KT (2003). Cinnamaldehyde induces apoptosis by ROS-mediated mitochondrial permeability transition in human pmmyelo-cytic leukemia HL-60 cells. *Cancer Lett.*, **19**(2): 143-152.

Küçüktürkmen B and Rosenholm JM (2021). Mesoporous silica nanoparticles as carriers for biomolecules in

cancer therapy. *Adv. Exp. Med. Biol.*, **1295**: 99-120.

Lai JP, Shah BR, Zhang YX, Yang LT and Lee KB (2015). Real-time monitoring of ATP-responsive drug release using mesoporous-silica-coated multicolor up-conversion nanoparticles. *ACS Nano.*, **9**(5): 5234-5245.

Li Q, Wang W, Hu G, Cui X, Sun D, Jin Z and Zhao K (2021). Evaluation of chitosan derivatives modified mesoporous silica nanoparticles as delivery carrier. *Molecules*, **24**: 2490.

Morsi DS, El-Nabi SH, Elmaghraby MA, Abu Ali OA, Fayad E, Khalifa SAM, El-Seedi HR, El-Garawani IM (2022). Anti-proliferative and immunomodulatory potencies of cinnamon oil on Ehrlich ascites carcinoma bearing mice. *Sci. Rep.*, **12**(1): 11839.

Padmajan Sasikala S, Poulin P and Aymonier C (2016). Prospects of supercritical fluids in realizing graphene-based functional materials. *Adv. Mater.*, **28**(14): 2663-91.

Srinivasarao M and Low P (2017). Ligand-targeted drug delivery. *Chem. Rev.*, **117**(19): 12133-12164.

Song YH, Li YH, Xu QE and Liu Z (2017). Mesoporous silica nanoparticles for stimuli-responsive controlled drug delivery: Advances, challenges and outlook. *Int. J. Nanomed. Nanosurg.*, **12**: 87-110.

Tukappa A, Ultimo A, De La Torre C and Pardo T (2016). Polyglutamic acid-gated mesoporous silica nano-particles for enzyme-controlled drug delivery. *Langmuir.*, **32**(33): 8507-8515.

Wang Y, Han N, Zhao QF, Bai L, Li J, Jiang TY and Wang SL (2015). Redox-responsive mesoporous silica as carriers for controlled drug delivery: A comparative study based on silica and PEG gatekeepers. *Eur. J. Pharm. Sci.*, **72**: 12-20.

Wen J, Yang K, Liu FY, Li HJ, Xu YQ and Sun SG (2017). Diverse gatekeepers for mesoporous silica nanoparticle based drug delivery systems. *Chem. Soc. Rev.*, **46**(19): 6024-6045.